Systematic functional characterization of resistance to PI3K inhibition in breast cancer

Xiuning Le*[1,2,3], Rajee Antony*[1,2], Pedram Razavi*[5,6], Daniel J. Treacy[1,2], Flora Luo[1,2], Mahmoud Ghandi[1,2], Pau Castel[5], Maurizio Scaltriti[5,7], Jose Baselga[5,6], Levi A. Garraway[1,2,4]

1. Department of Medical Oncology, Dana-Farber Cancer Institute, Boston, MA.

2. The Broad Institute of MIT and Harvard, Cambridge, MA.

3. Division of Hematology Oncology, Department of Medicine, Beth Israel Deaconess Medical Center, Boston MA

4. Department of Medicine, Brigham and Women's Hospital, Boston MA

5. Human Oncology and Pathogenesis Program, Memorial Sloan Kettering Cancer Center, New York, NY

6. Department of Medicine, Memorial Sloan Kettering Cancer Center, New York, NY

7. Department of Pathology, Memorial Sloan Kettering Cancer Center, New York, NY

* X.L., R.A., and P.R. contributed equally to this work

Corresponding author:

Levi A. Garraway, MD, PhD

Department of Medical Oncology,

Dana-Farber Cancer Institute,

44 Binney Street, D1542, Boston, MA, 02115

Tel: 617-632-6689

E-mail: levi_garraway@dfci.harvard.edu

Running Title:

Resistance to PI3K inhibition in breast cancer

Key words:

Breast cancer, Signal transduction pathways, Cell signaling, Protein serine-threonine kinases, Functional genomics, Oncogenes, Cellular responses to anticancer drugs, Novel mechanisms, Reversal of drug resistance, Kinase and phosphatase inhibitors

Disclosure of Potential Conflicts of interest:

L.A.G. is a consultant for Foundation Medicine, Novartis, Boehringer Ingelheim; an equity holder in Foundation Medicine; and a member of the Scientific Advisory Board at Warp Drive. L.A.G. receives sponsored research support from Novartis. Other authors declare no conflict of interest.

Abstract: *PIK3CA* (which encodes the phosphoinositide-3 kinase (PI3K) alpha isoform) is the most frequently mutated oncogene in breast cancer. Small-molecule PI3K inhibitors have shown promise in clinical trials; however, intrinsic and acquired resistance limits their utility. We used a systematic gain-of-function approach to identify genes whose upregulation confers resistance to the PI3K inhibitor BYL719 in breast cancer cells. Among the validated resistance genes, PIM kinases conferred resistance by maintaining downstream PI3K effector activation in an AKT-independent manner. Concurrent pharmacological inhibition of PIM and PI3K overcame this resistance mechanism. We also observed upregulated *PIM* expression and activity in a subset of breast cancer biopsies with clinical resistance to PI3K inhibitors. *PIM1* overexpression is mutually exclusive with *PIK3CA* mutation in treatment-naïve breast cancers, suggesting downstream functional redundancy. Together, these results offer new insights into resistance to PI3K inhibitors and support clinical studies of combined PIM/PI3K inhibition in a subset of *PIK3CA*-mutant cancers.

Statement of significance: PIM kinases overexpression confers resistance to small-molecule PI3K inhibitors. Combined inhibition of PIM and PI3K may therefore be warranted in a subset of breast cancers.

Introduction:

The phosphoinositide-3 kinase (PI3K) pathway represents an important oncogenic signaling network in breast cancer and other malignancies(1,2). PI3K signaling governs cell proliferation, cell cycle progression, and apoptosis, predominantly through phosphorylation of protein kinase B (also known as AKT) (3). *PIK3CA,* which encodes alpha isoform of the class I PI3K catalytic subunit, is one of the most commonly altered oncogenes in human cancer(4). Activating *PIK3CA* mutations and amplifications occur at high frequencies in cancers of the colon, lung (squamous), uterus, cervix, head/neck, and breast (5). In particular, over one third of invasive breast cancers harbor mutations in *PIK3CA*, most frequently in helical domain (e.g. E452K, E545K) and the catalytic domain (e.g. H1047R) (4,6).

The high prevalence of cancer-associated PI3K pathway alterations propelled the development of pharmacologic PI3K pathway inhibitors. As a result, several small molecules targeting class I PI3K isoforms are in clinical trials. BYL719 represents one such example: this drug selectively inhibits the alpha PI3K isoform (PI3Kα)(7). Multiple clinical trials are evaluating BYL719 for efficacy in breast cancers in combination with hormonal therapy, cytotoxic chemotherapy or cyclin-dependent kinase inhibitors (NCT01791478, NCT01300962, NCT01872260).

Although promising, BYL719 and other PI3K inhibitors have thus far only shown clinical efficacy in a relatively small subset of cancer patients. Moreover, the responses observed have generally been short-lived (8). Some of this lack of efficacy was due to toxicities of these drugs, but intrinsic and acquired resistance to PI3K inhibitors poses a significant clinical challenge in breast cancer and other malignancies. Recent studies have described several possible resistance mechanisms, including CDK4/6 activation (9), MYC amplification (10), enhanced estrogen receptor function (11), loss of PTEN(12), activation of PI3K p110β(13), and mTOR complex activation (14). In principle, systematic studies of resistance to PI3K inhibition should

improve our understanding of this drug resistance, which in turn could enable the emergence of more effective treatment strategies for many *PIK3CA*-mutant cancers.

Results:

A large-scale gain-of-function screen for resistance to PI3K inhibition

To identify a spectrum of genes whose upregulation confers resistance to PI3K inhibition, we expressed 15,970 human open reading frames (ORFs, corresponding to 13,229 genes) individually within breast cancer cells in the absence or presence of the PI3K inhibitor BYL719. For this screen we used T47D cells, which derive from the luminal A breast cancer subtype, harbor a *PIK3CA*^{H1047R} mutation, and are sensitive to BYL719. When these cells were infected with a lentivirus containing a myristoylated form of AKT (constitutively active, myr-AKT) (15), they developed profound resistance to BYL719 compared to negative controls (GFP-infected cells; Fig. 1A). Therefore, lentiviral GFP and myr-AKT were included in the screen (and thereafter) as negative and positive controls, respectively.

To carry out the primary screen, lentiviral supernatants containing individual ORFs were robotically arrayed into 384-well plates containing T47D cells. BYL719 or vehicle control (DMSO) was added the following day; each treatment was performed in duplicate. Cell viability was assessed by quantification of CellTiterGlo (CTG) after three days of drug exposure. As expected, BYL719 effectively suppressed T47D cell growth compared to vehicle controls; moreover, the duplicates showed excellent concordance (Fig. 1B). In total, 15,179 (95.05%) of ORFs met our infection efficacy criteria of greater than 65% (Supplementary Fig. S1A-B) and were subsequently analyzed for their effects on cell growth in the presence of BYL719. Seventy-three ORFs (corresponding to 63 genes) produced a robust Z-score of ≥ 2.5 and were considered as candidate resistance genes (Fig. 1C).

To validate these genes, we generated a customized library consisting of candidate ORFs together with a series of positive and negative controls. T47D cells were infected with this

library and cell growth was assessed at 10 different concentrations of BYL719 (0.003-32μM), including the 1.5μM condition used in the primary screen. At 1.5μM of BYL719, 60 of the 63 genes (95%) were confirmed to augment cell growth relative to controls. Next, the area under the curve (AUC) was calculated for each candidate gene using the full 10-point growth response curve data. Forty-five ORFs (corresponding to 43 genes) produced AUC values that exceeded a Z-score of 1.5 compared to controls (Fig. 1D and 1E). These were considered validated BYL719 resistance genes.

The PI3K inhibitor resistance genes encompass several known protein functional groups. *PDK1, AKT1* and *AKT2* represent isoforms of the major signaling effectors downstream of PI3K; thus, their validation as resistance genes *in vitro* supports the biological relevance of the screening results. Additionally, BYL719 resistance genes also exert known roles in signaling, including growth factors (*FGF3* and *FGF10*), G-protein coupled receptors (*GPR161*), GTPases/GEFs (*TBC1D3G*), tyrosine kinases (*SRC*), serine-threonine kinases (*PRKACA*), adapter proteins (*CRB3*), transcription factors/co-factors (*SMAD5* and *YAP1*), and others (Fig. 1D and Supplementary Table 1). Three BYL719 resistance genes (*AXL*, *CRKL*, and *YAP1*) were also identified previously as resistance genes to RAF/MEK inhibition in *BRAF*-mutant melanoma and ALK inhibition in *ALK*-rearranged lung cancer(16,17). These genes may therefore induce cell state changes that confer resistance to multiple targeted agents.

Interestingly, several PI3K resistance genes have an established association with obesity, suggesting mechanistic links between breast cancer and aberrant cell metabolism (Supplementary Table 1). For example, *DYRK1B* is a gene for which germ-line activating mutations (at codon R102C) predispose patients to early-onset diabetes and obesity, likely through enhanced adipogenesis (18). Similarly, *NUDT3* has also been implicated in multiple genome-wide association studies (GWAS) to be an obesity-linked gene (19,20). It is possible that overexpression of those genes may alter the metabolic profile to render cells less sensitive

to PI3K signaling. The recognition that these metabolic genes may impinge on oncogenic signaling cascades may offer new avenues to explore epidemiologic observations that obesity is a risk factor for breast cancer (21).

We next sought to determine whether any validated PI3K resistance genes might undergo dysregulation in human breast cancer. To assess this, we leveraged the TCGA breast cancer database (6) for which genomic and transcriptome data (RNA-seq) are available (22). TCGA copy-number analysis revealed that 7 resistance genes from our *in vitro* screens (FGF3, GPR161, TBC1D3G, CDK5R1, CCND1, SRP54, and PLEKHF1) were significantly amplified in breast cancer (GISTIC 2.0 analysis (23); Fig. 1F and Supplementary Table 2). To explore the candidate genes further in this context, we focused on a subset of candidate ORFs found to be amplified and/or overexpressed in human breast cancer (these are presumably of greatest clinical relevance) and tested whether they also conferred resistance in a second PIK3CA-mutant breast cancer cell line (MCF7, luminal A, $PIK3CA^{E545K}$) in the presence of GDC0941 (a distinct PI3Kα/δ inhibitor). We specifically prioritized the 7 genes with significant amplification (as assessed by GISTIC 2.0) and the 17 genes for which most TCGA tumor samples showed mRNA overexpression (5 genes were overlapping across these sets; Supplementary Methods). Among the set of 19 genes having amplification and/or overexpression in human tumors, 11 conferred resistance to GDC0941 in MCF7 cells (Fig. 1F). Thus, at least some of the validated resistance genes extend to distinct cellular and pharmacologic contexts.

PIM kinases confer resistance to PI3K inhibition in breast cancer cells

Two isoforms of the Proviral Insertion site in Murine leukemia virus (PIM) protein kinase family (PIM1 and PIM3) conferred robust growth in the presence of BYL719. PIM kinases are highly conserved serine/threonine kinases that have been shown to be overexpressed in hematological malignancies and prostate cancers (24). Small-molecule PIM kinase inhibitors have entered clinical development for hematological malignancies (25,26); however, their role in

breast cancer remains poorly understood. PIM kinases have been implicated in the regulation of apoptosis, metabolism, and the cell cycle (24,26). Several of these functions overlap with those of PI3K/AKT signaling. Because of the strong PIM kinase resistance phenotype and the availability of pharmacological inhibitors in clinical trials, we sought to determine whether PIM kinases might mediate a generalizable and clinically tractable PI3K inhibitor resistance mechanism.

To test this possibility, we first examined whether the PIM kinase resistance phenotype might be generalizable to other breast cancer cell lines and PI3K pathway inhibitors. Here, we overexpressed PIM1 in breast cancer cell lines representative of various molecular subtypes (luminal A and B, HER2-enriched, and basal-like) and generated BYL719 response curves. These cell lines also harbored a range of *PIK3CA* and *PTEN* genetic alterations. PIM1 overexpression conferred resistance across multiple contexts, including luminal A (MCF7 and EFM19), luminal B (BT474), and HER2-amplified (HCC202, MDAMB453) subtypes (Fig. 2A, Supplementary Fig. S2A-C and Supplementary Table 3 and 4). HCC1419 is a luminal B cell line that lacks *PIK3CA* mutations; therefore, in these cells PIM1 increased the GI_{50} to a lesser extent than in cell lines with *PIK3CA* mutation (Supplementary Fig. S2D). Two cell lines with *PTEN* loss of function: HCC1937 (basal-like subtype with homozygous *PTEN* deletion) and MDAMB415 (luminal subtype with $PTEN^{C136Y}$ mutation and diminished PTEN expression) were resistant to BYL719 at baseline (GI_{50} >10uM, Supplementary Fig. S2E), consistent with prior reports that breast cancer cells lacking PTEN are insensitive to PI3K pathway inhibition(12,27). Taken together, these observations suggest that PIM1-mediated resistance may be generalizable across various breast cancer contexts.

We also examined pharmacologic inhibitors of various PI3K pathway components (Supplementary Material and References), including additional PI3K inhibitors (GDC0941 and BKM120), two PI3K/mTOR dual inhibitors (GDC0032 and PI-103), two PDK1 inhibitors (BX795 and BX912), two AKT inhibitors (MK2206 and GDC0068), two mTOR allosteric inhibitors

(Sirolimus and Everolimus) and two mTOR catalytic inhibitors (PP242 and WYE). PIM1 conferred resistance to all of these inhibitors (Fig. 2B and Supplementary Fig. S3A-F) with the exception of the PDK1 inhibitor BX912 and the PI3K/mTOR inhibitor PI-103. Of note, BX912 demonstrated poor efficacy in T47D cells at baseline (GI_{50}>200uM). Thus, PIM1 overexpression confers resistance to PI3K pathway inhibition across multiple pharmacologic contexts.

Although *PIM2* was not identified as a resistance gene in the primary screen, we reasoned that the resistance phenotype should also extend to this isoform. To assess this, we overexpressed each PIM kinase isoform (PIM1, PIM2, and PIM3) in T47D cells and cultured the resulting populations in the absence or presence of BYL719. Here, we examined the resistance phenotype using both short-term (3 days) cell growth inhibition assays and longer-term (3 weeks) colony formation assays. The effects of PIM2 and PIM3 on BYL719 pharmacologic GI_{50} values were more modest than that of PIM1 in these short-term assays (PIM1 increased the GI_{50} value by 4.71-fold, PIM2 by 2.45-fold, PIM3 by 1.30-fold, respectively; Fig. 2C and Supplementary Table 4). However, all three kinases conferred a robust BYL719 resistance effect in colony-formation assays (Fig. 2D). Thus, overexpression of each PIM kinase isoform was capable in principle of producing resistance to PI3K inhibition.

PIM1 activates PI3K downstream effectors in an AKT-independent manner

Many targeted therapy resistance mechanisms engender re-activation of the downstream signaling pathway governed by the target oncoprotein (28); however, pathway-independent resistance mechanisms have also been described (29). To ascertain if PIM-mediated resistance requires AKT activation, we determined its effect on PI3K pathway activity by measuring AKT phosphorylation following PIM1 overexpression in the absence or presence of PI3K inhibitors. In T47D cells, PIM1 overexpression had only minimal effects on AKT(S473) phosphorylation compared to controls (Fig. 3A). Moreover, AKT(S473) phosphorylation remained suppressed in both control (GFP) and PIM1 expressing cells in the presence of PI3K

inhibitor treatments (Fig. 3A). These data suggest that PIM-mediated resistance to PI3K inhibitors does not require AKT activation.

Since the consensus PIM phosphorylation motif (L/KRRXS*/T*) (30) is similar to that of AKT (RXRXXS*/T*), PIM1 and AKT share common phosphorylation targets, including the proline-rich Akt substrate of 40 kDa PRAS40(T246), Bcl2-associated death promoter BAD(S112), $p21^{CIP/WAF1}$ (T145) and $p27^{Kip1}$(T157, Supplementary Table 5) (31–34). We therefore hypothesized that PIM1 might mediate resistance to PI3K inhibition by activating downstream effectors common to both PIM and AKT kinases. To test this, we first examined the effect of PIM1 overexpression on phosphorylation levels of two targets shared by PIM1 and AKT: PRAS40(T246) and BAD(S112). In control (GFP) T47D cells, PRAS40(T246) phosphorylation was readily detected and only minimally affected by PIM1 or myr-AKT overexpression (Fig.3B lane 7,13 vs.1). In the presence of BYL719; however, PRAS40(T246) phosphorylation was suppressed in control (GFP) cells but maintained at high levels in PIM1- and myr-AKT-overexpressing cells (Fig 3B lanes 2,3 vs. 8,9 and 14,15). BAD(S112) phosphorylation, which was relatively low in GFP control cells, was robustly augmented by both PIM1 and myr-AKT overexpression. As seen with PRAS40(T246), the elevated BAD(S112) phosphorylation observed in this setting was not suppressed by BYL719 (Fig. 3B, lanes 2,3 vs. 8,9 and 14,15). These results supported the notion that PIM1 overexpression might exert resistance to PI3K inhibition in part by activating downstream effectors that are normally regulated by AKT.

Phosphorylation of PRAS40(T246) results in its dissociation from mTOR complex 1 (mTORC1), thereby relieving an inhibitory constraint on mTOR activity. In turn, this promotes mTOR-dependent translation initiation and protein synthesis. Given that PIM1 overexpression produces sustained PRAS40(T246) phosphorylation in the setting of PI3K inhibition, we reasoned that PIM1 might maintain mTOR activation and drive continued protein translation in the presence of PI3K inhibition. To test this, we measured the phosphorylation levels of several mTOR pathway components in control (GFP), PIM1 and myr-AKT overexpressing cells. In the

absence or presence of PI3K inhibition, phosphorylation levels of p70S6K1(T389) and 4EBP(T37/46), two direct mTOR targets, were unaffected by BYL719, indicating that mTOR activity was maintained in the setting of PIM1 overexpression despite PI3K inhibition (Fig. 3B, lane 8,9 vs. 2,3). Phosphorylation of RPS6(S235/236), which correlates with the output of translation initiation, showed similar effects (Fig. 3B, lane 8,9). Taken together, these results support a mechanism in which PIM1 overexpression bypasses AKT but phosphorylates PRAS40 and other downstream effectors. This leads to mTOR-dependent protein translation in the presence of PI3K inhibition.

Having established that PIM1 overexpression maintains effector activities downstream of PI3K, we next sought to determine whether pharmacological inhibition of PIM1 could reverse this signaling activation. For this, we obtained two small-molecule PIM inhibitors (LGH447 and AZD1208) currently in clinical trials for certain hematological malignancies (35,36). Single-agent PIM inhibition had only a minimal growth inhibitory effect in either control T47D (GFP) cells or T47D cells with PIM1 overexpression (Supplementary Fig. S4A-B). We measured the effects of LGH447 on PIM1-mediated PRAS40(T246) and BAD(S112) phosphorylation in the presence of BYL719. In T47D cells, single-agent inhibition with either BYL719 (from 0.3-1μM, Fig. 3B lanes 8,9) or LGH447 (1μM, lane 10), failed to suppress PIM1-driven PRAS40(T246) and BAD(S112) phosphorylation; however, concurrent PIM/PI3K inhibition achieved robust suppression of those effectors (Fig. 3B, lane 12). In contrast, single-agent BYL719 (from 0.3-1μM) suppressed both PRAS40(T246) and BAD(S112) phosphorylation in control (GFP) cells (Fig. 3B lanes 2,3). Moreover, dual PIM/PI3K inhibition effectively suppressed p70 S6K1(T389), 4EBP(T37/46) and RPS6(S235/236) phosphorylation, indicating a reduction in mTOR signaling output (Fig. 3B, lane 10). We note that even combined PIM/PI3K inhibition did not reverse myr-AKT-mediated PRAS40(T246) and BAD(S112) phosphorylation (Fig. 3B, lanes 17,18) — this is not surprising given the known supra-physiological effect of AKT myristoylation on downstream signaling. Taken together, these data provided further support to the notion that PIM1 overexpression

maintains the activity of key downstream effectors that are typically enacted by AKT kinases, but suppressed by PI3K inhibition.

PIM kinases are perhaps best known for their cell cycle regulatory roles (24,26). In this regard, the cell cycle regulators $p21^{CIP/WAF1}$ and $p27^{Kip1}$ comprise two additional phosphorylation targets common to both PIM1 and AKT kinases (Supplementary Table 5). Thus, in addition to the effects of PIM kinases on protein translation, we also sought to determine if cell cycle regulation might also play a role in PIM-mediated resistance to PI3K inhibition. To assess this, we performed cell cycle analysis on control (GFP) or PIM1 overexpressing cells in the presence or absence of PI3K or PIM inhibitors. In control (GFP) cells, treatment with BYL719 significantly decreased the percentage of cells in S phase (2.9 ± 0.1% with BYL719 versus 28.1 ± 0.32% with DMSO, $p < 0.01$) as expected (Fig. 3C). PIM1 overexpression by itself produced a small increase in S phase cells compared to GFP controls (31.6 ± 1.2% in PIM1 versus 28.1% ± 0.32 in GFP expressing cells; Fig. 3C, DMSO treated group). In the presence of BYL719, PIM1 overexpression maintained a higher percentage of cells in S phase (17.2 ± 1.1% in PIM1 versus 2.9 ± 0.1% in GFP expressing cells, $p< 0.01$, Fig 3C, BYL719 treated group). When LGH447 was combined with BYL719 in PIM1 expressing cells, the percentage of cells in S phase was again suppressed (9.2 ± 0.9% compared to 17.2 ± 1.1% in BYL719 treatment alone ($p< 0.01$) and 22.3 ± 0.3 % in LGH447 treatment alone ($p<0.01$), Fig. 3C and Supplementary Fig. S5). These data indicate that PIM1 overexpression abrogates the cell cycle inhibitory effects of BYL719 and raise the possibility that the PIM kinase effect on cell cycle may also contribute to the resistance phenotype.

In prostate cancer cells, inhibition of AKT has been shown to induce PIM1 upregulation (37). We therefore hypothesized that PIM kinases might also become upregulated after PI3K inhibition in breast cancer cells, and that this in turn might promote resistance to PI3K inhibition. To test this hypothesis, we utilized T47D cells that had been cultured to resistance through prolonged exposure to BYL719. Here, T47D cells were grown in increasing concentrations of

BYL719 until the proliferation rate of the resulting population in the presence of BYL719 (1μM) was comparable to that of parental T47D cells (14). Immunoblotting studies were performed on both parental (T47D) and resistant (T47DR) cells after treatment with BYL719 (1μM) for 0, 4 and 24 hours (Fig 3D). Phosphorylation of AKT(S473) was effectively inhibited in both parental and resistant (T47DR) cells (Fig. 3D), suggesting an AKT-independent resistance mechanism. Notably, the levels of PIM1, PIM2, and PIM3 proteins were elevated in T47DR cells compared to parental (drug-sensitive) T47D cells. Moreover, phosphorylation levels of downstream effectors including PRAS40(T246), RPS6(S240/4244), and BAD(S112) were maintained in the T47DR cells, suggesting that mTOR-dependent protein translation and BAD associated anti-apoptosis were maintained in those cells. This data suggests that PIM kinases can be induced following prolonged *in vitro* exposure to BYL719, thereby providing an independent line of evidence that these kinases may mediate resistance to PI3K inhibition.

PIM inhibition enhances sensitivity to BYL719 in *PIK3CA*-mutant cancer cells with elevated PIM1 expression

Given that ectopic expression of PIM1 confers resistance to PI3K inhibition, we hypothesized that endogenous PIM1 might be associated with intrinsic resistance to PI3K inhibition. To investigate this possibility, we first looked for a correlation between PIM1 expression and BYL719 sensitivity in *PIK3CA*-mutant breast cancer cell lines. For this analysis, we queried the Cancer Cell Line Encyclopedia (38) and identified 15 *PIK3CA*-mutant breast cancer cell lines. In a prior study, GI_{50} values for BYL719 were determined for 13 of these 15 lines (14). We binned these cell lines into “sensitive (9 lines) and “resistant” (4 lines) categories using a BYL719 GI_{50} threshold of 1μM. Indeed, the four resistant cell lines showed elevated PIM1 expression compared to the sensitive group (mean PIM1 log2 mRNA expression level = 7.51 +/- 0.29 in the resistant cell lines versus 5.82 +/- 0.55 in the sensitive cell lines, p=0.00015). Thus, PIM1 expression was inversely associated with BYL719 sensitivity in this

dataset (Fig. 4A). The PIM2 and PIM3 mRNA expression levels did not show statistical association with BYL719 sensitivity (Supplementary Table 6).

If high endogenous PIM1 confers biologically meaningful resistance to BYL719 in cancer cell lines, small-molecule PIM inhibitors should (at least partially) reverse the resistance phenotype. To address this possibility, we first sought to confirm that pharmacologic PIM inhibition could reverse the resistance effects of PIM1 overexpression in breast cancer cells. We generated dose response curves for BYL719 in the absence and presence of PIM inhibitors (LGH447 or AZD1208). PIM inhibitors restored BYL719 sensitivity in PIM1 overexpressing cells, whereas they had little effect in GFP control cells (Fig. 4B and Supplementary Fig. S6A-B). We also performed colony-formation assays to validate this effect. Here, combined BYL719/AZD1208 and BYL719/ LGH447 exposure strongly suppressed cell growth in these assays when compared to single agents or vehicle controls. In contrast, concurrent treatment of BYL719 with a MEK inhibitor (trametinib) had no effect on the PIM1 mediated resistance to BYL719, suggesting that the reversal of BYL719 resistance is specific to PIM inhibition (Fig. 4C). Thus, PIM inhibitors effectively reverse the PIM1-dependent resistance phenotype in cells with exogenous PIM1 overexpression, as expected.

Next, we tested whether PIM inhibitors could sensitize *PIK3CA*-mutant breast cancer cells with high endogenous PIM1 expression to PI3K inhibitors. We generated BYL719 dose response curves in the presence or absence of the PIM inhibitor LGH447 using representative cell lines with high (CAL51, HCC1954, JIMT-1, BT20) or low PIM1 expression (T47D and EFM19), respectively. LGH447 (1μM) significantly decreased the BYL719 GI_{50} in 3 out of 4 cell lines with high endogenous *PIM1* expression: CAL51 (by 2.5-fold), JIMT1 (by 4-fold) and HCC1954 (by 2.5-fold); but not BT20 cells (Fig. 4D and Supplementary Table 7). LGH447 did not significantly alter BYL719 sensitivity in the control cell lines with low endogenous *PIM1* expression (T47D and EFM19; Fig 4D and Supplementary Table 7). We confirmed these observations using colony-formation assays in CAL51 and JIMT1 cells (Fig. 4E). Together,

these data support the notion that high PIM1 expression may reduce the intrinsic sensitivity of *PIK3CA*-mutant cancer cells to PI3K inhibition, but this effect can often be mitigated *in vitro* through combined PIM/PI3K inhibition.

We also asked whether the mechanism of reduced sensitivity to PI3K inhibition observed in *PIK3CA*-mutant cells with high endogenous PIM1 might also occur through a convergence of PIM signaling onto downstream effectors common to PI3K/AKT activation. This was assessed using immunoblotting studies of salient downstream effectors. In CAL51, JIMT1 and HCC1954 cells, single-agent BYL719 suppressed AKT(S473) phosphorylation effectively at 1μM; however, phosphorylation of PRAS40(T246), RPS6(S235/236) and BAD(S112) remained robust. However, combined PIM/PI3K inhibition effectively suppressed PRAS40(T246), RPS6(S235/236) and BAD(S112) phosphorylation in these cells (Fig 4F). In contrast, phosphorylation of PRAS40(T246), RPS6(S235/236) and BAD(S112) were sufficiently suppressed by BYL719 alone in (drug-sensitive) T47D cells. Taken together, these results suggest that high endogenous PIM1 reduces sensitivity to PI3K inhibition in at least some breast cancer cell lines through sustained activation of downstream PI3K/AKT effectors.

PI3K resistance genes are upregulated in breast tumor biopsies after BYL719 treatment

To determine if any resistance genes identified by our systematic functional approach might promote clinical resistance to PI3K inhibition, we obtained breast tumor tissue biopsies from a small collection of patients treated with BYL719 as part of a clinical trial. Patients in this trial had advanced estrogen-receptor positive, HER2 negative (ER+/HER2-) breast cancers and received prior hormonal therapy. Each patient underwent a biopsy before initiation of BYL719 together with either letrozole or exemestane (treatment-naïve biopsy, TN). Some patients also received additional post-relapse biopsies as they were going off study–usually because of either progressive disease (PD) or toxicity (TX). RNA was prepared from formalin-fixed paraffin-embedded (FFPE) tissue samples, and RNA-sequencing (RNA-seq) was performed. In total, we

obtained evaluable RNA-seq data in paired biopsies from six patients (Table 1). However, in Pt 6 the second biopsy was taken only 14 days after initiation of BYL719; and in Pt 3 the second biopsy was taken after the patient developed intolerable toxicity and went off study (Table 1). Thus, for this analysis of resistance gene effects we used paired treatment-naïve and post-relapse RNA-seq data from four patients (Pt 1, 2, 4, 5).

First, we asked whether any validated PI3K resistance genes we identified showed upregulation in a post-relapse sample compared to its treatment-naïve counterpart. In five patients with paired biopsies, a subset of PI3K resistance genes from this study showed increased expression in the second biopsy specimen (four of these were post-relapse cases, as noted above; Fig 5A). The panel of validated resistance genes from our functional screens tended to be overexpressed in the drug-resistant breast tumor samples (p-value=0.01). The expression differences in these genes observed between treatment-naïve and drug-resistant tumors failed to reach statistical significance due to the small sample set. In particular, AKT2, CRKL, and PIM1 upregulation were each observed in two patients (AKT2: Pt1 and Pt 2, CRKL: Pt 2 and Pt 3, and PIM1: Pt 3 and Pt 4; Fig 5A). AKT1 was also upregulated in Pt 2 (Fig. 5A). In Pt 6, the second biopsy was a short interval biopsy, as described above. In this case, candidate gene transcripts from the pre- and on-treatment biopsies did not show discernible changes, as expected given that the tumor had not progressed to drug resistance. Though preliminary, these observations were consistent with the premise that a subset of resistance genes identified through our functional screens *in vitro* might contribute to understanding clinical resistance to PI3K inhibition in breast cancer.

We next investigated whether PIM activation or upregulation might be associated with clinical resistance in some cases. To facilitate this, we generated a PIM expression signature in T47D cells by comparing RNA-seq-based expression profiles of cells with PIM1 overexpression to control (GFP-expressing) cells and uninfected parental cells. The top 37 differentially upregulated genes together with PIM1, 2, 3, and the top 47 differentially downregulated genes

(FDR<10%) were defined as a PIM activation signature (Supplementary Fig. S7). Using this signature, we applied single-sample gene set enrichment analysis (ssGSEA) (17) to generate an enrichment score in each post-relapse sample relative to its treatment-naïve pair. Among the four biopsy pairs that were informative, the PIM signatures was upregulated in two pairs (Pt 4 and Pt 5, solid lines, red and dark red, Fig. 5B) when compared to the remaining pair-wise comparisons (t-test p=0.02). Both PIM1 and PIM3 transcripts were themselves upregulated in Pt 4, in addition to the PIM activation signature. PIM3 appeared modestly upregulated in the Pt 5 post-relapse sample, although the abundance of PIM3 was low in both biopsies (Fig. 5A and Supplementary Table 8 and Supplementary Methods). Interestingly, the other two informative tumor sample pairs (Pt 1 and Pt 2, solid line, blue and light blue, Fig. 5B) showed AKT2 upregulation by RNA-seq in the post-relapse setting compared to treatment-naïve biopsies, as noted above. Although the sample size is small, this observation raised the possibility that AKT upregulation might also contribute to resistance (as might be expected given its known signaling function downstream of PI3K). Overall, these observations provide initial support for the notion that PIM upregulation might be associated with clinical resistance to BYL719 in a subset of patients. Other mechanisms of resistance--for example, AKT upregulation--might also contribute to tumor progression in this treatment context.

PIM family genes are amplified or overexpressed in treatment-naïve human breast tumors

Since PIM and AKT can signal to common downstream effectors (as shown above), we hypothesized that activation of these kinases might generally exhibit a mutually exclusive pattern in human breast cancer. Initial support for this notion was discernible in the paired treatment-naïve and post-relapse biopsies from the BYL719 clinical trial, where the two cases with PIM activation were distinct from those with AKT mRNA upregulation (Fig. 5A). To investigate this possibility in a larger tumor cohort, we assessed the prevalence of PIM kinase dysregulation in human breast cancers and compared this to somatic genetic activation of the

PI3 kinase pathway using the TCGA breast invasive carcinoma database (provisional; (6)). In this dataset, both genomic and transcriptome data (RNA-seq) are available for analysis. Among 960 treatment-naïve tumors, 74 (7.7%) cases showed either *PIM1* copy-number gain/amplification or mRNA overexpression (Supplementary Table 9). *PIM1, PIM2,* or *PIM3* are altered in 135 of the 960 cases (14%) in this cohort. Among these 135 cases, 125 showed copy-number gain/-amplification or mRNA overexpression of at least one PIM gene. We noted that *PIM1* and *PIM2* alterations tended to co-occur (p=0.001, log odd ratio=1.335), as did *PIM1* and *PIM3* alterations (p=0.014, log odd ratio=1.164, Supplementary Fig. S8A). Interestingly, *PIM1* amplification/mRNA overexpression exhibited a pattern that mutual exclusive with *PIK3CA* alterations (mutations, amplification or mRNA overexpression; p<0.001,log odd ratio= -0.904, Fig. 5C and Supplementary Fig. S8B).

To investigate this further, we grouped all cases bearing PIM family gene alterations into a single “PIM dysregulated group” (135 cases) and those with *PIK3CA* and/or *PTEN* alterations into a “PI3K pathway dysregulatd group” (465 cases). We observed a statistically significant mutual exclusivity (p=0.0015, log odd ratio =-0.6165) between those two groups in this cohort (Supplementary Fig. S8A and S8C). These data are consistent with the hypothesis that dysregulated PIM kinases exert cellular functions that show at least partial functional redundancy with oncogenic PI3K pathway alterations. In some cases, this functional redundancy may conceivably become exploited as a resistance mechanism to PI3K inhibition.

Discussion:

PIK3CA is the most commonly mutated oncogene in breast cancer (6) and frequently sustains activating mutations in several other tumor types. Therefore, small-molecule PI3K inhibitors are currently being evaluated in multiple clinical trials—often in combination with other anticancer drugs. However, intrinsic and acquired resistance to PI3K inhibitors has limited their clinical benefit. Understanding the mechanisms by which cancer cells evade PI3K inhibition may

speed the development of new therapeutic strategies in *PIK3CA*-mutant breast cancer and other PI3K-dependent tumors.

In the past, our group has successfully utilized systematic functional approaches to identify a range of resistance mechanisms to targeted therapies (16,17). Here, we applied a similar gain-of-function approach to characterize resistance to PI3K inhibition in breast cancer. Our screen identified both known and novel resistance genes to PI3K inhibition. PDK1 and AKT represent clear examples of known pathway-dependent resistance mechanisms. The AXL receptor tyrosine kinase offers another example: this kinase has been reported to mediate resistance to PI3K inhibition in *PIK3CA*-mutant head and neck squamous cell carcinomas (39). These findings affirm the ability of large-scale functional screens to reveal biologically and clinically relevant drug resistance mechanisms.

Our approach also uncovered genes that have not been directly associated with resistance to PI3K targeted therapies. One example is SRC, a non-receptor tyrosine kinase and "classic" viral oncogene (40). Because SRC has been shown to constitutively activate PI3K/AKT signaling (41), it is likely that overexpression of SRC may also confer resistance to PI3K inhibition in a PI3K/AKT pathway-dependent fashion; however, this remains to be confirmed experimentally. Another group of intriguing resistance genes are the metabolic genes, for example, DYRK1B and NUDT3. Gain-of-function mutation in DYRK1B resulted in an inherited form of the metabolic syndrome in patients (18). NUDT3 is particularly associated with obesity in females (19,20). However, specific mechanisms through which alteration of metabolic profiles might confer resistance to PI3K inhibition in cancer remain uncharacterized. These and other PI3K resistance genes validated *in vitro* may also provide new insights into links between adipogenesis and glucose homeostasis that impinge on PI3K signaling.

The discovery that PIM kinases confer robust resistance to PI3K inhibition *in vitro* is of interest given that PIM kinase inhibitors are in clinical development for other malignancies. Although the PIM kinase family members share high protein homology and functional

redundancy, they have divergent tissue distributions. PIM1 is highly expressed in hematopoietic cells, as well as breast and cervical epithelia. In contrast, PIM2 is mainly expressed in the spleen and lymphoid cells, and PIM3 is expressed in the kidney, breast, and brain tissue (24). PIM kinases become overexpressed in a wide variety of human tumors of both hematological and epithelial origin (26). PIM kinases exert multiple cellular functions through phosphorylation-dependent regulation of many substrate proteins. Well-known functions of PIM kinases include regulation of cell cycle progression through the cell cycle inhibitors p21 and p27, apoptosis through BAD and MDM2, and translation through PRAS40. Given the similarity of the consensus phosphorylation motifs between PIM1 and AKT, it is not surprising that both kinase families may exert partially overlapping oncogenic signaling effects in different cell contexts (42–44). Indeed, our results indicate that phosphorylation levels of several substrate proteins common to both AKT and PIM kinases (e.g., PRAS40 and BAD) are maintained by PIM overexpression in a manner refractory to PI3K inhibition. These findings suggest that PIM signaling confers resistance to PI3K inhibition in part through bypass of AKT itself but convergence onto downstream AKT effector mechanisms.

Additional evidence that PIM and AKT may share functional redundancy in cancer emerged from our analysis of the TCGA breast cancer database. This analysis revealed a statistical mutual exclusivity of *PIM1* amplification/overexpression and *PIK3CA* mutation in human breast cancers, thereby providing genetic evidence that these signaling pathways may converge onto common biological outputs. Therefore, the PIM1 resistance mechanism characterized here may represents a pathway bypass-based cancer drug resistance mechanism that bears similarity to MET amplification in resistance to EGFR therapy in lung cancer (29) and COT expression in resistance to RAF inhibition in melanoma (45).

Unlike many other protein kinases, PIM kinases are constitutively active and are not thought to be regulated by phosphorylation. In the hematopoietic compartment, they are controlled at the transcriptional level by the JAK/STAT pathway (46). In MCF7 breast cancer

cells, several ER-binding regions (ERBs) were found as enhancers of *PIM1* expression. Moreover, PIM1 was shown to be an estrogen receptor target (47). Here, we demonstrated that breast cancer cells cultured to PI3K inhibitor resistance also exhibited induction of PIM signaling and an AKT-independent resistance mechanism. Toward this end, prior work has also raised the possibility that other effectors might also produce AKT-independent signals downstream of PI3K. For example, serum and glucocorticoid-induced kinase 3 (SGK3) may exert such a role in *PIK3CA*-mutant cells that are less reliant on AKT for survival (48). Although the molecular details of how PI3K/AKT inhibition may induce PIM1 expression remain incompletely characterized, PI3K inhibition is known to induce ER signaling (11). Thus, it is conceivable that upregulation of estrogen-induced kinases (which include both PIM1 and SGK3) (48,49) provides a common mechanism for breast cancer cells to reduce their dependency on PI3K/AKT signaling.

In breast cancer, *PIK3CA* has the highest mutational rate in the luminal and HER2-amplified subtypes. Most clinical trials of PI3K inhibitors were therefore designed to target these subtypes, often in combination with anti-estrogen or anti-HER2 therapies. We showed that PIM1 overexpression confers resistance to a variety of breast cancer cell lines with different *PIK3CA* mutations and different intrinsic subtypes (Fig 2A and Supplementary Fig S2). We also found that PIM1 overexpression occurs across multiple genetic/molecular subtypes in human breast tumors (Supplementary Table 7). Previous reports that PIM1 and PIM2 were identified as resistance drivers to anti-HER2 treatment in breast cancer cells (50) provide additional evidence that PIM kinases may function as resistance drivers when a HER2-PI3K oncogenic signaling module is operant. Taken together, our findings suggest that PIM kinase-mediated resistance to PI3K inhibition may conceivably attenuate multiple therapeutic contexts in breast cancer.

The ultimate validation for any cancer drug resistance mechanism involves confirmation of its role in the clinical setting. Such studies typically require paired treatment-naïve and drug-resistant tumor samples from the same patient. Accordingly, our study also included an analysis

of biopsies obtained from breast cancer patients enrolled in a BYL719 clinical trial. Here, it should be noted that large numbers of patient-derived pre-treatment and post-relapse biopsy pairs are often unavailable prior to FDA approval of the drug in question. The results gleaned using RNA-seq data obtained from a small number of paired breast cancer biopsies from patients treated with BYL719 in combination with hormonal therapy must therefore be considered preliminary. Nonetheless, these cases offer some support to the notion that PIM upregulation may promote acquired resistance to PI3K inhibition in the clinic. Specifically, 2 out of 4 patients who developed resistance to BYL719 showed PIM transcript upregulation and/or PIM signature enrichment in their drug-resistant biopsy. Moreover, the two drug-resistant tumors that did not have PIM upregulation harbored elevated expression of one or more AKT isoforms, again supporting the notion of functional redundancy between these effects during clinical resistance to PI3K inhibition.

The transcriptome analysis of this tumor biopsy cohort is also consistent with the notion that resistance to PI3K inhibition may be heterogeneous, with multiple mechanisms conceivably operant within the same tumor locus. In all post-resistant cases analyzed, multiple validated resistance genes showed measurable upregulation after BYL719 treatment. Such heterogeneity may pose a significant challenge when considering the design of therapeutic combinations capable of overcoming cancer drug resistance. Future studies of larger drug-resistant cohorts are needed to better delineate the spectrum of clinically relevant PI3K resistance mechanisms and guide rational design of parsimonious therapeutic combinations that achieve more lasting disease control.

In summary, the integration of systematic experimental studies with mechanistic and clinical analyses has defined a diverse molecular landscape of resistance to PI3K inhibition in breast cancer cells. In particular, PIM kinases upregulation may comprise one clinically relevant resistance mechanism that is therapeutically actionable in the near term. More generally, our results suggest that the use of large-scale functional and clinical datasets paired with detailed

knowledge of tumor biology may enable the discovery of new therapeutic avenues that help circumvent the challenge of drug resistance in many cancer types.

Methods:

Cell lines and chemical reagents:

T47D, MCF7 cells were purchased from American Type Culture Collection (ATCC) in 2012 - 2015. They were authenticated using STR testing and tested negative for *Mycoplasma* contamination. EFM19, BT474, MDAMB453, HCC202, MDAMB361, HCC1419, MDAMB415, HCC1937, CAL51, BT20, HCC1954, and JIMT1 cells were purchased from Cancer Cell Line Encyclopedia (CCLE) at the Broad Institute in 2015-2016, and were authenticated using SpectroCHIPII-G384 by Sequenom's MassARRAY Analyzer Compact. All the cells were maintained in RPMI-1640 with 10% fetal bovine serum. BYL719, GDC0941, BKM120, AZD1208, GDC0032, PI-103, BX795, BX912, MK2204, GDC0068, sirolimus, everolimus, PP242 and WYE were purchased from Selleck Chemicals (Supplementary Material and Methods). Blasticidine was purchased from Life Technologies. LGH447 was obtained from Novartis.

Open-reading frame (ORF) lentiviral expression screen:

The CCSB-Broad lentiviral expression library was described previously. T47D cells were seeded into 384-well plates at 700 cells per well. Twenty-four hours after seeding, the ORF lentivirus with polybrene (4μg/ml) was added to each well individually for infection and followed by a spin at 2,250 rpm for 30 minutes at 37°C. Cells were infected with each ORF in five replicates. On the next day, media with lentivirus was removed and changed to fresh media. Subsequently, BYL719 or DMSO was added at 1.5μM final concentration for treatment in duplicates. Blasticidin (40μg/ml) was added for selection to the fifth replicate plate. All the treated plates were incubated at 37°C for 72 hours. The cell viability was assessed by robotic quantification of CellTiterGlo assay (Promega). The entire screen was performed in six batches. Cell seeding, lentiviral infection, media change, chemical addition were performed by robots.

Western immunoblotting:

Anti-phospho-AKT (S473), anti-total AKT, anti-phospho-PRAS40 (T246), anti-phospho-S6K1 (T389), anti-4EBP (T37/46), anti-phospho-S6 ribosomal protein (S235/236 or S240/244), and anti-phospho-BAD (S112) were purchased from Cell Signaling. Anti-vinculin antibody was purchased from EMD Millipore. The use of secondary antibodies, dilution of primary antibodies and blocking were performed according to the manufacturer's recommendations. Cell lysates were prepared using RIPA buffer (Sigma) with proteinase inhibitor (Roche) and phosphatase inhibitor (Roche). Lysate with SDS sample buffer were subjected to SDS-PAGE (Novex) followed by blotting onto nitrocellulose membrane. SuperSignal west chemiluminescent detection reagents were used (ThermoFisher Scientific).

RNA-sequencing in tumor samples:

Patient tumor samples were obtained under a protocol approved by the Memorial Sloan Kettering Cancer Center (MSKCC) Institutional Review Board (IRB), and all participating patients provided written informed consent. The studies were conducted in accordance with the Declaration of Helsinki. Total RNA was extracted from formalin-fixed, paraffin-embedded (FFPE) tumor specimens using AllPrep DNA/RNA Kit (QIAGEN) according to the manufacturer's instructions. Total RNA was assessed for quality using the Caliper LabChip GX2. The percentage of fragments with a size greater than 200nt (DV200) was calculated using software. An aliquot of 200ng of RNA was used as the input for first strand cDNA synthesis using Illumina's TruSeq RNA Access Library Prep Kit. Synthesis of the second strand of cDNA was followed by indexed adapter ligation. Subsequent PCR amplification enriched for adapted fragments. The amplified libraries were quantified using an automated PicoGreen assay. 200ng of each cDNA library, not including controls, were combined into 4-plex pools. Capture probes that target the exome were added, and hybridized for recommended time. Following hybridization, streptavidin magnetic beads were used to capture the library-bound probes from the previous step. Two wash steps effectively remove any non-specifically

bound products. These same hybridization, capture and wash steps are repeated to assure high specificity. A second round of amplification enriches the captured libraries. After enrichment the libraries were quantified with qPCR using the KAPA Library Quantification Kit for Illumina Sequencing Platforms and then pooled equimolarly. The entire process is in 96-well format and all pipetting is done by either Agilent Bravo or Hamilton Starlet. Pooled libraries were normalized to 2nM and denatured using 0.1 N NaOH prior to sequencing. Flowcell cluster amplification and sequencing were performed according to the manufacturer's protocols using HiSeq 2500. Each run was a 76bp paired-end with an eight-base index barcode read. Data was analyzed using the Broad Picard Pipeline, which includes de-multiplexing and data aggregation.

TCGA dataset analysis

The cBioPortal (www.cbioportal.org) was utilized for analysis and visualization of invasive breast cancer dataset. Specifically, in the query, the Breast Invasive Carcinoma (TCGA Provisional) was selected under Cancer Study; Mutations, Putative copy-number alterations from GISTIC and mRNA expression data (mRNA expression by RNA Seq V2 RSEM, overexpression as measured by a z-score >2.0 compared to the expression of each gene in tumors that are diploid for this gene by RNA-seq) were selected under Genomic Profiles; PIM1, PIM2, PIM3, PIK3CA and PTEN were entered under Gene Set. OncoPrint figures were downloaded for visualization in Fig 5 and Supplementary Fig S7A. The number of cases harboring each mutation was counted manually (Supplementary Fig S7B and S7C).

Statistical analysis

In cell cycle analysis, unpaired t-test was used to compare percentage of cells in S phase between two conditions (Fig 3C). In the analysis to detect association between endogenous PIM expression and BYL719 resistance in various breast cancer cell lines, unpaired t-test was used to calculate the p value (Fig 4A). We subsequently defined PIM1 log2 mRNA expression ≥7.0 as high endogenous level, and < 7 as low. In the patient samples, gene expression RPKM values for the 6 post-treatment samples were transformed to z-scores. A gene with a z-score

greater than 1 was defined as over expressed. The total number of over expressed genes in the 6 post-treatment samples was used as the test statistic, and a permutation test with N=100,000 permutations was applied. p = 0.01. An ssGSEA score was calculated for each biopsy sample (see supplementary methods.) The differential ssGSEA score between the second biopsy and treatment-naïve biopsy was calculated for each patient sample pair. Pt 4 and Pt 5 had upregulation of the ssGSEA scores and grouped together. The rest of the four differential scores were used for comparison. Unpaired t-test was used (Fig 5B). Mutual exclusivity analysis was performed using a 2x2 contingency table. Fisher's exact test was used for calculation of p value. Log odd ratio was calculated for tendency of co-occurrence /mutual exclusivity (Fig 5C and supplementary Fig S6).

Acknowledgements:

We thank the Novartis PIM447 group for general sharing of reagents; Eva Goetz, Lior Golomb, Alison Taylor and Christopher Salthouse for helpful discussion and critical review of the manuscript; and Federica Piccioni, Mutka Bagul, Bokang Rabasha, Rachel Leeson for technical assistance. We thank all the Garraway lab members for helpful discussion.

Grant support:

This work was supported by National Cancer Institute R35 CA197737 (L.A.G.), P30 CA0087748, R01CA190642-01A1 (J.B.), Starr Cancer Consortium (L.A.G.), Gerstner Foundation (L.A.G.), DFCI-NOVARTIS Drug Discovery Program (L.A.G.), Claudia Adams Barr Program for Innovative Cancer Research (X.L.), Stand Up To Cancer (SU2C) and the V foundation (TVF) Scholar Award (X.L.), American Society of Clinical Oncology (ASCO) Young Investigator Award (X.L.), Peter and Deborah Weinberg Family Fund (P.R.), Breast Cancer Research Foundation (Tory Burch Award, M.S) and the Geoffrey Beene Cancer Research Center (M.S.).

References:

1. Wong K-K, Engelman JA, Cantley LC. Targeting the PI3K signaling pathway in cancer. Curr Opin Genet Dev. 2010 Feb;20(1):87–90.

2. Baselga J. Targeting the phosphoinositide-3 (PI3) kinase pathway in breast cancer. The Oncologist. 2011;16 Suppl 1:12–9.

3. Cantley LC. The phosphoinositide 3-kinase pathway. Science. 2002 May 31;296(5573):1655–7.

4. Samuels Y, Wang Z, Bardelli A, Silliman N, Ptak J, Szabo S, et al. High frequency of mutations of the PIK3CA gene in human cancers. Science. 2004 Apr 23;304(5670):554.

5. Vivanco I, Sawyers CL. The phosphatidylinositol 3-Kinase–AKT pathway in human cancer. Nat Rev Cancer. 2002 Jul;2(7):489–501.

6. Cancer Genome Atlas Network. Comprehensive molecular portraits of human breast tumours. Nature. 2012 Oct 4;490(7418):61–70.

7. Fritsch C, Huang A, Chatenay-Rivauday C, Schnell C, Reddy A, Liu M, et al. Characterization of the novel and specific PI3Kα inhibitor NVP-BYL719 and development of the patient stratification strategy for clinical trials. Mol Cancer Ther. 2014 May;13(5):1117–29.

8. Juric D, Rodon J, Gonzalez-Angulo A, Baselga J. Abstract CT-01: BYL719, a next generation PI3K alpha specific inhibitor: Preliminary safety, PK, and efficacy results from the first-in-human study. In: Proceedings of the 103rd Annual Meeting of the American Association for Cancer Research; 2012 Mar 31-Apr 4; Chicago, IL. Philadelphia (PA): AACR; Cancer Res 2012;72(8 Suppl):Abstract nr CT-01.

9. Vora SR, Juric D, Kim N, Mino-Kenudson M, Huynh T, Costa C, et al. CDK 4/6 inhibitors sensitize PIK3CA mutant breast cancer to PI3K inhibitors. Cancer Cell. 2014 Jul 14;26(1):136–49.

10. Ilic N, Utermark T, Widlund HR, Roberts TM. PI3K-targeted therapy can be evaded by gene amplification along the MYC-eukaryotic translation initiation factor 4E (eIF4E) axis. Proc Natl Acad Sci U S A. 2011 Sep 13;108(37):E699–708.

11. Bosch A, Li Z, Bergamaschi A, Ellis H, Toska E, Prat A, et al. PI3K inhibition results in enhanced estrogen receptor function and dependence in hormone receptor-positive breast cancer. Sci Transl Med. 2015 Apr 15;7(283):283ra51.

12. Juric D, Castel P, Griffith M, Griffith OL, Won HH, Ellis H, et al. Convergent loss of PTEN leads to clinical resistance to a PI(3)Kα inhibitor. Nature. 2015 Feb 12; 518(7538):240-4.

13. Costa C, Ebi H, Martini M, Beausoleil SA, Faber AC, Jakubik CT, et al. Measurement of PIP3 levels reveals an unexpected role for p110β in early adaptive responses to p110α-specific inhibitors in luminal breast cancer. Cancer Cell. 2015 Jan 12;27(1):97–108.

14. Elkabets M, Vora S, Juric D, Morse N, Mino-Kenudson M, Muranen T, et al. mTORC1 inhibition is required for sensitivity to PI3K p110α inhibitors in PIK3CA-mutant breast cancer. Sci Transl Med. 2013 Jul 31;5(196):196ra99.

15. Kohn AD, Summers SA, Birnbaum MJ, Roth RA. Expression of a Constitutively Active Akt Ser/Thr Kinase in 3T3-L1 Adipocytes Stimulates Glucose Uptake and Glucose Transporter 4 Translocation. J Biol Chem. 1996 Dec 6;271(49):31372–8.

16. Johannessen CM, Johnson LA, Piccioni F, Townes A, Frederick DT, Donahue MK, et al. A melanocyte lineage program confers resistance to MAP kinase pathway inhibition. Nature. 2013 Dec 5;504(7478):138–42.

17. Wilson FH, Johannessen CM, Piccioni F, Tamayo P, Kim JW, Van Allen EM, et al. A functional landscape of resistance to ALK inhibition in lung cancer. Cancer Cell. 2015 Mar 9;27(3):397–408.

18. Keramati AR, Fathzadeh M, Go G-W, Singh R, Choi M, Faramarzi S, et al. A form of the metabolic syndrome associated with mutations in DYRK1B. N Engl J Med. 2014 May 15;370(20):1909–19.

19. Goumidi L, Cottel D, Dallongeville J, Amouyel P, Meirhaeghe A. Effects of established BMI-associated loci on obesity-related traits in a French representative population sample. BMC Genet. 2014;15:62.

20. Kitamoto A, Kitamoto T, Mizusawa S, Teranishi H, So R, Matsuo T, et al. NUDT3 rs206936 is associated with body mass index in obese Japanese women. Endocr J. 2013;60(8):991–1000.

21. James FR, Wootton S, Jackson A, Wiseman M, Copson ER, Cutress RI. Obesity in breast cancer--what is the risk factor? Eur J Cancer Oxf Engl 1990. 2015 Apr;51(6):705–20.

22. Cerami E, Gao J, Dogrusoz U, Gross BE, Sumer SO, Aksoy BA, et al. The cBio cancer genomics portal: an open platform for exploring multidimensional cancer genomics data. Cancer Discov. 2012 May;2(5):401–4.

23. Mermel CH, Schumacher SE, Hill B, Meyerson ML, Beroukhim R, Getz G. GISTIC2.0 facilitates sensitive and confident localization of the targets of focal somatic copy-number alteration in human cancers. Genome Biol. 2011;12(4):R41.

24. Narlik-Grassow M, Blanco-Aparicio C, Carnero A. The PIM family of serine/threonine kinases in cancer. Med Res Rev. 2014 Jan;34(1):136–59.

25. Burger MT, Nishiguchi G, Han W, Lan J, Simmons R, Atallah G, et al. Identification of N-(4-((1R,3S,5S)-3-Amino-5-methylcyclohexyl)pyridin-3-yl)-6-(2,6-difluorophenyl)-5-fluoropicolinamide (PIM447), a Potent and Selective Proviral Insertion Site of Moloney Murine Leukemia (PIM) 1, 2, and 3 Kinase Inhibitor in Clinical Trials for Hematological Malignancies. J Med Chem. 2015 Nov 12;58(21):8373–86.

26. Warfel NA, Kraft AS. PIM kinase (and Akt) biology and signaling in tumors. Pharmacol Ther. 2015 Jul;151:41–9.

27. Weigelt B, Warne PH, Downward J. PIK3CA mutation, but not PTEN loss of function, determines the sensitivity of breast cancer cells to mTOR inhibitory drugs. Oncogene. 2011 Jul 21;30(29):3222–33.

28. Emery CM, Vijayendran KG, Zipser MC, Sawyer AM, Niu L, Kim JJ, et al. MEK1 mutations confer resistance to MEK and B-RAF inhibition. Proc Natl Acad Sci U S A. 2009 Dec 1;106(48):20411–6.

29. Engelman JA, Zejnullahu K, Mitsudomi T, Song Y, Hyland C, Park JO, et al. MET amplification leads to gefitinib resistance in lung cancer by activating ERBB3 signaling. Science. 2007 May 18;316(5827):1039–43.

30. Peng C, Knebel A, Morrice NA, Li X, Barringer K, Li J, et al. Pim kinase substrate identification and specificity. J Biochem (Tokyo). 2007 Mar;141(3):353–62.

31. Zhang Y, Wang Z, Magnuson NS. Pim-1 kinase-dependent phosphorylation of p21Cip1/WAF1 regulates its stability and cellular localization in H1299 cells. Mol Cancer Res MCR. 2007 Sep;5(9):909–22.

32. Aho TLT, Sandholm J, Peltola KJ, Mankonen HP, Lilly M, Koskinen PJ. Pim-1 kinase promotes inactivation of the pro-apoptotic Bad protein by phosphorylating it on the Ser112 gatekeeper site. FEBS Lett. 2004 Jul 30;571(1-3):43–9.

33. Wang Z, Bhattacharya N, Mixter PF, Wei W, Sedivy J, Magnuson NS. Phosphorylation of the cell cycle inhibitor p21Cip1/WAF1 by Pim-1 kinase. Biochim Biophys Acta. 2002 Dec 16;1593(1):45–55.

34. Morishita D, Katayama R, Sekimizu K, Tsuruo T, Fujita N. Pim kinases promote cell cycle progression by phosphorylating and down-regulating p27Kip1 at the transcriptional and posttranscriptional levels. Cancer Res. 2008 Jul 1;68(13):5076–85.

35. Keeton EK, McEachern K, Dillman KS, Palakurthi S, Cao Y, Grondine MR, et al. AZD1208, a potent and selective pan-Pim kinase inhibitor, demonstrates efficacy in preclinical models of acute myeloid leukemia. Blood. 2014 Feb 6;123(6):905–13.

36. Garcia P, Langowski J, Holash J, Burger M, Zang R, Zavorotinskaya T, et al. The Pan-PIM Kinase Inhibitor LGH447 Shows Activity In PIM2-Dependent Multiple Myeloma and In AML Models. ASH 2013; 122:1666

37. Cen B, Mahajan S, Wang W, Kraft AS. Elevation of receptor tyrosine kinases by small molecule AKT inhibitors in prostate cancer is mediated by Pim-1. Cancer Res. 2013 Jun 1;73(11):3402–11.

38. Barretina J, Caponigro G, Stransky N, Venkatesan K, Margolin AA, Kim S, et al. The Cancer Cell Line Encyclopedia enables predictive modelling of anticancer drug sensitivity. Nature. 2012 Mar 29;483(7391):603–7.

39. Elkabets M, Pazarentzos E, Juric D, Sheng Q, Pelossof RA, Brook S, et al. AXL mediates resistance to PI3Kα inhibition by activating the EGFR/PKC/mTOR axis in head and neck and esophageal squamous cell carcinomas. Cancer Cell. 2015 Apr 13;27(4):533–46.

40. Wheeler DL, Iida M, Dunn EF. The Role of Src in Solid Tumors. The Oncologist. 2009 Jul 1;14(7):667–78.

41. Chen R, Kim O, Yang J, Sato K, Eisenmann KM, McCarthy J, et al. Regulation of Akt/PKB Activation by Tyrosine Phosphorylation. J Biol Chem. 2001 Aug 24;276(34):31858–62.

42. Meja K, Stengel C, Sellar R, Huszar D, Davies BR, Gale RE, et al. PIM and AKT kinase inhibitors show synergistic cytotoxicity in acute myeloid leukaemia that is associated with convergence on mTOR and MCL1 pathways. Br J Haematol. 2014 Oct;167(1):69–79.

43. Walpen T, Kalus I, Schwaller J, Peier MA, Battegay EJ, Humar R. Nuclear PIM1 confers resistance to rapamycin-impaired endothelial proliferation. Biochem Biophys Res Commun. 2012 Dec 7;429(1-2):24–30.

44. Hammerman PS, Fox CJ, Birnbaum MJ, Thompson CB. Pim and Akt oncogenes are independent regulators of hematopoietic cell growth and survival. Blood. 2005 Jun 1;105(11):4477–83.

45. Johannessen CM, Boehm JS, Kim SY, Thomas SR, Wardwell L, Johnson LA, et al. COT drives resistance to RAF inhibition through MAP kinase pathway reactivation. Nature. 2010 Dec 16;468(7326):968–72.

46. Yip-Schneider MT, Horie M, Broxmeyer HE. Transcriptional induction of pim-1 protein kinase gene expression by interferon gamma and posttranscriptional effects on costimulation with steel factor. Blood. 1995 Jun 15;85(12):3494–502.

47. Malinen M, Jääskeläinen T, Pelkonen M, Heikkinen S, Väisänen S, Kosma V-M, et al. Proto-oncogene PIM-1 is a novel estrogen receptor target associating with high grade breast tumors. Mol Cell Endocrinol. 2013 Jan 30;365(2):270–6.

48. Vasudevan KM, Barbie DA, Davies MA, Rabinovsky R, McNear CJ, Kim JJ, et al. AKT-Independent Signaling Downstream of Oncogenic PIK3CA Mutations in Human Cancer. Cancer Cell. 2009 Jul 7;16(1):21–32.

49. Wang Y, Zhou D, Phung S, Masri S, Smith D, Chen S. SGK3 is an estrogen-inducible kinase promoting estrogen-mediated survival of breast cancer cells. Mol Endocrinol Baltim Md. 2011 Jan;25(1):72–82.

50. Moody SE, Schinzel AC, Singh S, Izzo F, Strickland MR, Luo L, et al. PRKACA mediates resistance to HER2-targeted therapy in breast cancer cells and restores anti-apoptotic signaling. Oncogene. 2015 Apr 16;34(16):2061–71.

Table 1. Clinical characteristics of tumor samples from patients who underwent BYL719 treatment.

Patient ID	Status	Biopsy site	Second biopsy status
1	TN	breast	Progression of disease
	PD	liver	
2	TN	liver	Progression of disease
	PD	liver	
3	TN	breast skin	Toxicity
	TX	breast skin	
4	TN	abdominal wall	Progression of disease
	PD	skin	
5	TN	breast	Progression of disease
	PD	liver	
6	TN	liver	Stable disease
	SD	liver	

TN: treatment-naïve, PD: progression of disease, TX: toxicity, SD: stable disease.

Legends:

Figure 1. A large-scale gain-of-function screen for resistance to PI3K inhibition. A. T47D cells, T47D cells expressing GFP or myrAKT were treated with various doses of BYL719 for 3 days. Cell proliferation was determined by MTS assay. Mean and SE of three replicates are shown. **B.** Cell viability (expressed as absolute CellTiterGlo values) for all assayed ORFs in the presence of BYL719 versus DMSO in duplicate. **C.** The screening hits are visualized by plotting the function y = z-score, x = gene name. The representative candidate genes are indicated. **D.** Heat map displaying validation results of all 63 genes. Top row was validation at original screening drug dose. Bottom row was the normalized area under the curve (AUC) for each candidate genes with 10-point drug concentration. The genes were organized by their protein functional groups. GPCR, G-protein coupled receptor; GEF, guanine nucleotide exchange factors. **E.** Summary of primary screening and validation studies: 43 genes were validated in T47D cells after 10-point concentration test. **F.** TCGA amplification and overexpression status of 19 candidates genes and heatmap displaying validation results of these genes in T47D cells using BYL719 and MCF7 cells using GDC0941.

Figure 2. PIM kinases confer resistance to PI3K inhibitors in breast cancer cells. A. T47D, MCF7, BT474, and MDAMB453 cells expressing GFP, PIM1, or myrAKT were treated with various doses of BYL719 for 3 days. Cell proliferation was determined by MTS assay. Mean and SE of three replicates are shown. **B.** T47D cells expressing GFP, PIM1, and myrAKT were treated with various doses of BYL719, GDC0941, MK2206, or GDC0068 for 3 days. Cell proliferation was determined by MTS assay. Mean and SE of three replicates are shown. **C.** T47D cells expressing PIM1, PIM2, or PIM3 were treated with various doses of BYL719 for 3 days. Cell proliferation was determined by MTS assay. Mean and SE of three replicates are shown. **D.** T47D cells expressing PIM1, PIM2, or PIM3 were treated with DMSO or BYL719

(0.5μM) for 21 days followed by staining with crystal violet. Media was changed with fresh drug addition every 3 days.

Figure 3. PIM1 confers resistance through activating common downstream pathways of AKT in the presence of PI3K inhibition. A. T47D cells expressing GFP or PIM1 were treated with the indicated inhibitors (each at 1μM concentration) for 24 hours, and cell lysates were prepared for immunoblotting for the indicated proteins. **B.** T47D cells expressing GFP, PIM1, or myrAKT were treated with the indicated inhibitors (BYL719 at 0, 0.3, and 1μM, LGH447 at 1μM) for 24 hours, and cell lysates were prepared for immunoblotting for the indicated proteins. **C.** T47D cells with indicated treatment were fixed in ethanol for cell cycle analysis. Percent of S phase cells were shown. Mean and SE of three replicates are shown. ** indicates $p<0.01$. **D.** T47D cells cultured to resistance in the presence of BYL719. Both parental (T47D) and resistant (T47DR) cells were treated with BYL719 at 1μM, and cell lysates were prepared at 0, 4, 24 hours for immunoblotting for the indicated proteins.

Figure 4. Inhibition of PIM enhances the sensitivity to BYL719 in cell lines with high endogenous PIM1. A. *PIK3CA*-mutant breast cancer cell lines were classified to resistant to BYL719 (GI_{50}>1μM) and sensitive to BYL719. Their PIM1 expression levels (log2) were plotted on y-axis. ** indicates $p<0.01$. **B** T47D cells expressing GFP or PIM1 were treated with various doses of BYL719 in the presence or absence of LGH447 (1μM) for 3 days. Cell proliferation was determined by MTS assay. Mean and SE of three replicates are shown. **C.** T47D cells expressing PIM1 or GFP were treated with DMSO, BYL719 (0.5μM), BYL719 (0.5μM) + AZD1208 (1μM), BYL719 (0.5μM)+LGH447 (0.5μM), BYL719 (0.5μM) + trametinib (0.1μM) for 21 days followed by staining with crystal violet. Media was changed with fresh drug addition every 3 days. **D.** CAL51, HCC1954, JIMT1, BT20, T47D and EFM19 cells were treated with various doses of BYL719 in the presence or absence of LGH447 (1μM) for 3 days. Cell

proliferation was determined by MTS assay. Mean and SE of three replicates are shown. **E.** CAL51 and JIMT1 cells were treated with DMSO, BYL719 (1μM), LGH447 (1μM) and BYL719 (1μM) +LGH447 (1μM) for 21 days followed by staining with crystal violet. Media was changed with fresh drug addition every 3 days. **F.** T47D, CAL51, JIMT1 and HCC1954 cells were treated with the indicated inhibitors (BYL719 at 1μM and LGH447 at 1μM) for 24 hours, and cell lysates were prepared for immunoblotting for the indicated proteins.

Figure 5. Resistance genes are upregulated in clinical breast tumor biopsies after BYL719 treatment. A. Heatmap representation of relative transcript abundance of each validated resistance genes in each patient sample pairs. Red: high abundance; blue: low abundance. PD: progression of disease, TN: treatment-naïve, TX: toxicity, SD: stable disease **B.** Graphical representation of the PIM signature in the tumor samples. **C.** Matrix heatmap generated using cBioPortal showing genetic alterations of *PIM1* and *PIK3CA* in the breast invasive carcinoma (TCGA, provisional) dataset (only part of the whole dataset was shown).

Figure 1

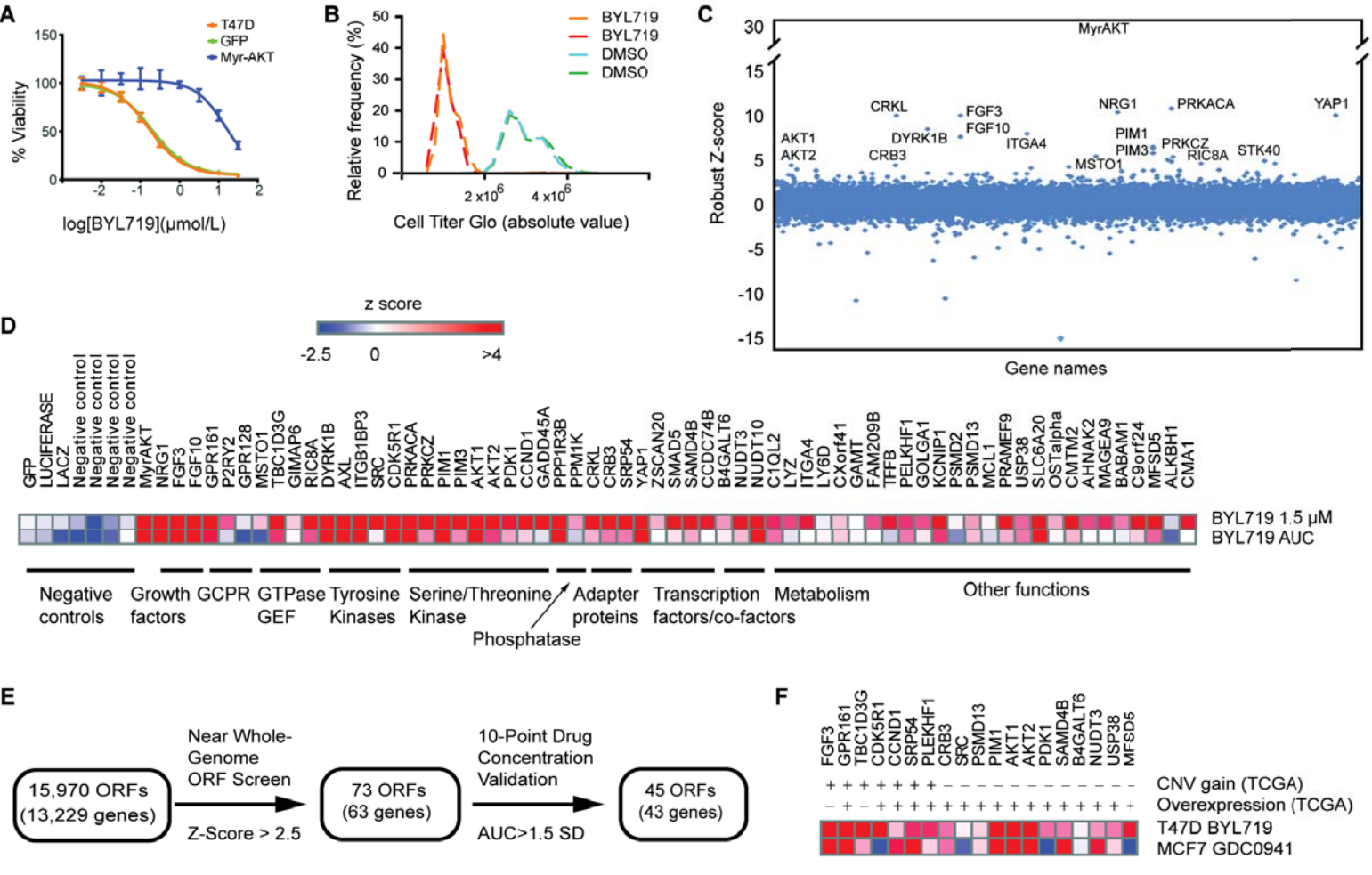
A
T47D
GFP
Myr-AKT
% Viability
log[BYL719](μmol/L)
B
BYL719
BYL719
DMSO
DMSO
Relative frequency (%)
Cell Titer Glo (absolute value)
C
MyrAKT
Robust Z-score
Gene names
AKT1
AKT2
CRB3
CRKL
DYRK1B
FGF3
FGF10
ITGA4
MSTO1
NRG1
PIM1
PIM3
PRKACA
PRKCZ
RIC8A
STK40
YAP1
D
z score
-2.5
0
>4
BYL719 1.5 μM
BYL719 AUC
Negative controls
Growth factors
GCPR
GTPase GEF
Tyrosine Kinases
Serine/Threonine Kinase
Phosphatase
Adapter proteins
Transcription factors/co-factors
Metabolism
Other functions
E
15,970 ORFs (13,229 genes)
Near Whole-Genome ORF Screen
Z-Score > 2.5
73 ORFs (63 genes)
10-Point Drug Concentration Validation
AUC>1.5 SD
45 ORFs (43 genes)
F
CNV gain (TCGA)
Overexpression (TCGA)
T47D BYL719
MCF7 GDC0941

Figure 2

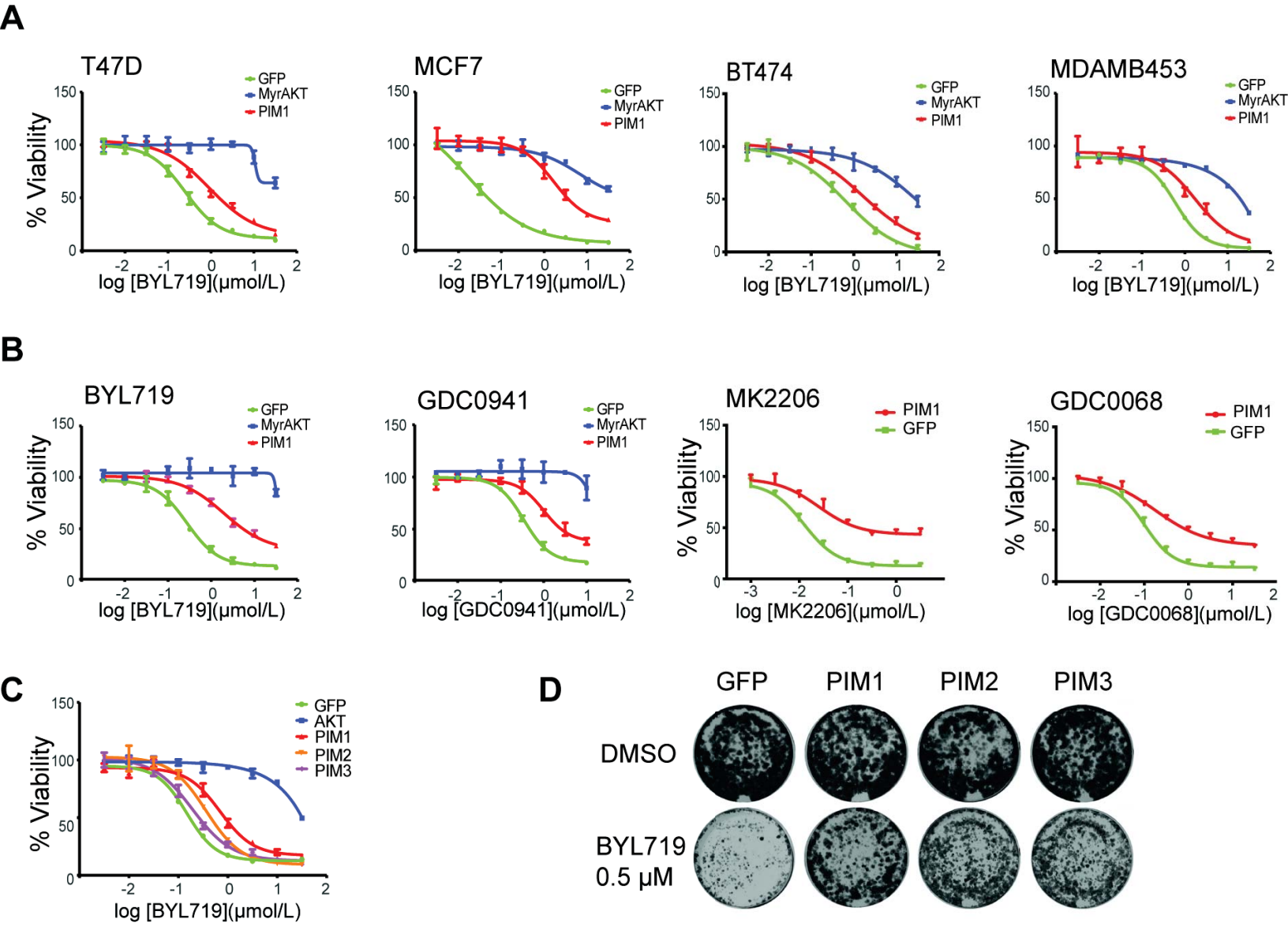
A
T47D
MCF7
BT474
MDAMB453
GFP
MyrAKT
PIM1
% Viability
log [BYL719](μmol/L)
B
BYL719
GDC0941
MK2206
GDC0068
PIM1
GFP
log [GDC0941](μmol/L)
log [MK2206](μmol/L)
log [GDC0068](μmol/L)
C
AKT
PIM2
PIM3
D
DMSO
BYL719
0.5 μM

Figure 3

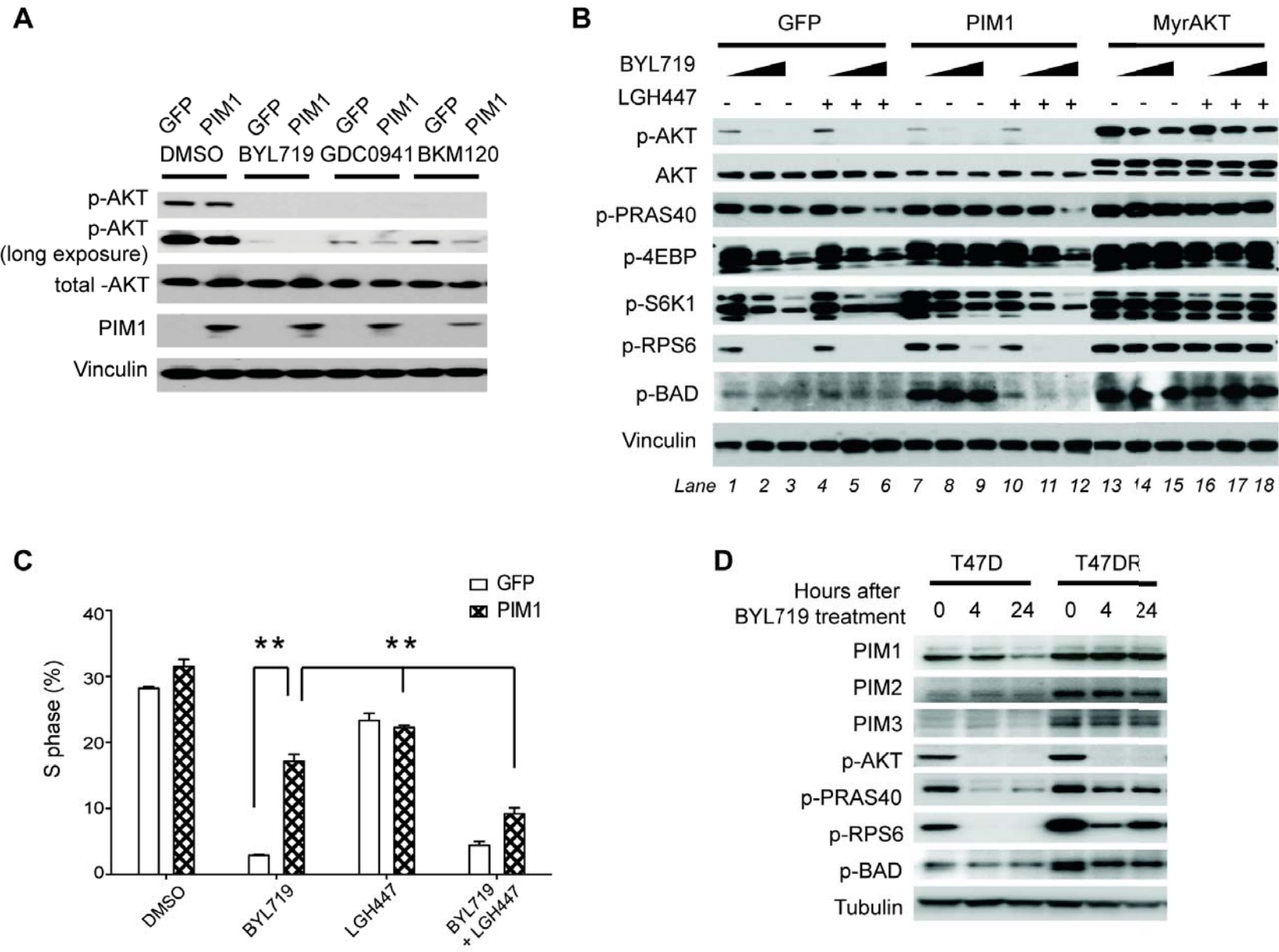
A
GFP
PIM1
DMSO
BYL719
GDC0941
BKM120
p-AKT
p-AKT (long exposure)
total -AKT
PIM1
Vinculin
B
GFP
PIM1
MyrAKT
BYL719
LGH447
p-AKT
AKT
p-PRAS40
p-4EBP
p-S6K1
p-RPS6
p-BAD
Vinculin
Lane 1 2 3 4 5 6 7 8 9 10 11 12 13 14 15 16 17 18
C
GFP
PIM1
S phase (%)
40
30
20
10
0
**
**
DMSO
BYL719
LGH447
BYL719 + LGH447
D
T47D
T47DR
Hours after BYL719 treatment
0 4 24 0 4 24
PIM1
PIM2
PIM3
p-AKT
p-PRAS40
p-RPS6
p-BAD
Tubulin

Figure 4

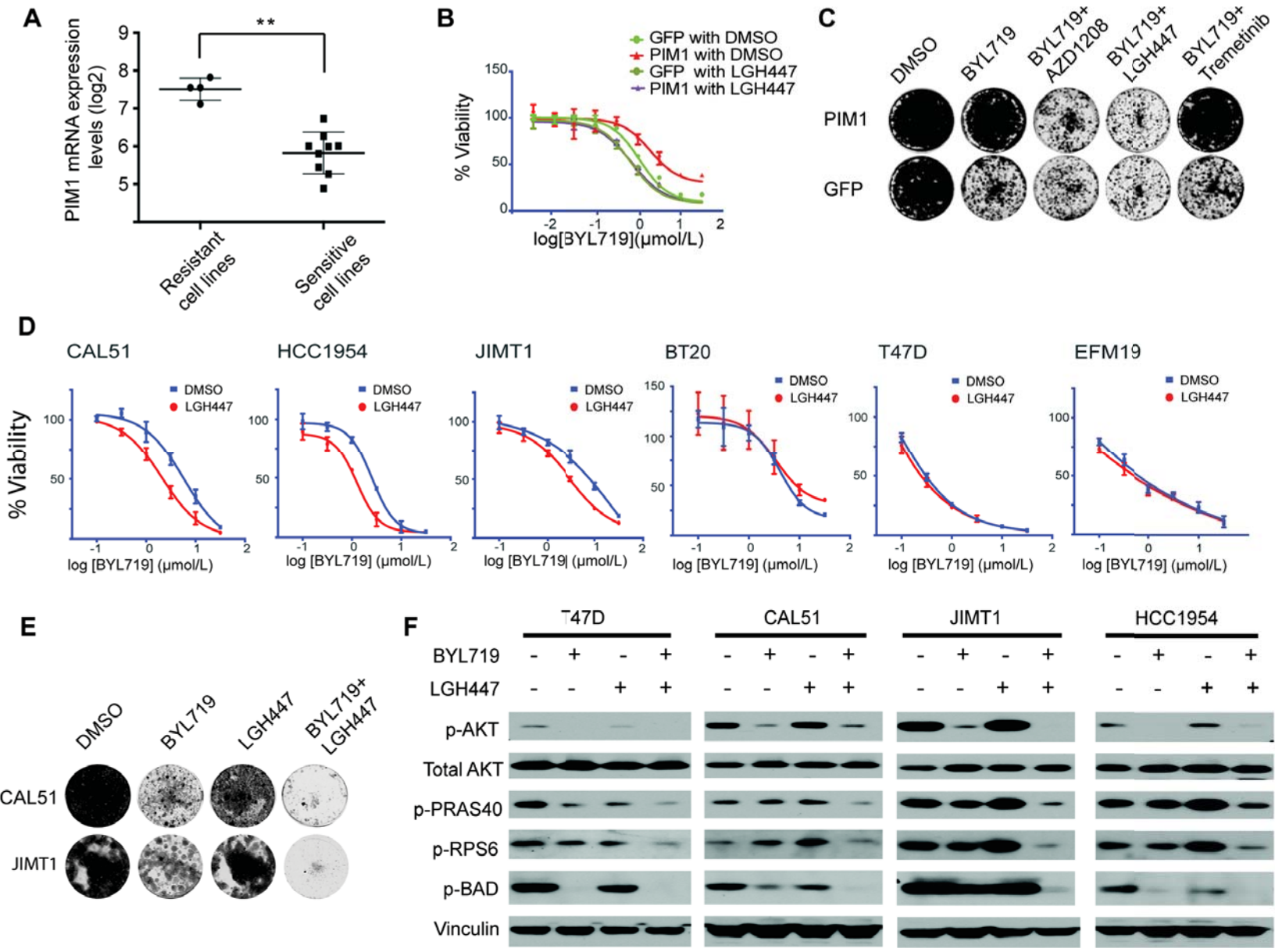
A
PIM1 mRNA expression levels (log2)
**
Resistant cell lines
Sensitive cell lines
B
GFP with DMSO
PIM1 with DMSO
GFP with LGH447
PIM1 with LGH447
% Viability
log[BYL719](μmol/L)
C
DMSO
BYL719
BYL719+ AZD1208
BYL719+ LGH447
BYL719+ Trametinib
PIM1
GFP
D
CAL51
HCC1954
JIMT1
BT20
T47D
EFM19
DMSO
LGH447
% Viability
log [BYL719] (μmol/L)
E
DMSO
BYL719
LGH447
BYL719+ LGH447
CAL51
JIMT1
F
T47D
CAL51
JIMT1
HCC1954
BYL719
LGH447
p-AKT
Total AKT
p-PRAS40
p-RPS6
p-BAD
Vinculin

Figure 5

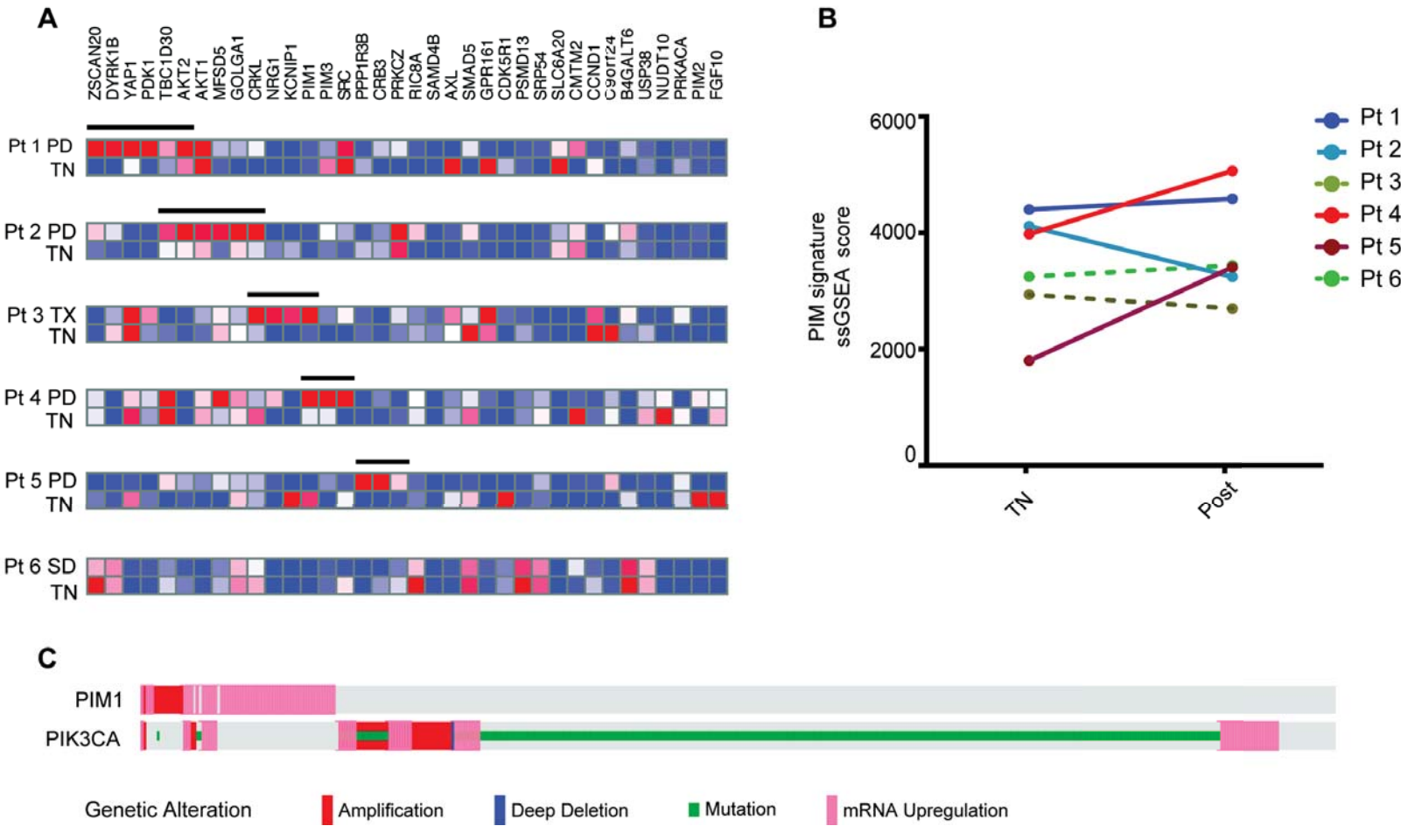
A
ZSCAN20
DYRK1B
YAP1
PDK1
TBC1D30
AKT2
AKT1
MFSD5
GOLGA1
CRKL
NRG1
KCNIP1
PIM1
PIM3
SRC
PPP1R3B
CRB3
PRKCZ
RIC8A
SAMD4B
AXL
SMAD5
GPR161
CDK5R1
PSMD13
SRP54
SLC6A20
CMTM2
CCND1
B4GALT6
USP38
NUDT10
PRKACA
PIM2
FGF10
Pt 1 PD
TN
Pt 2 PD
TN
Pt 3 TX
TN
Pt 4 PD
TN
Pt 5 PD
TN
Pt 6 SD
TN
B
PIM signature ssGSEA score
6000
4000
2000
0
TN
Post
Pt 1
Pt 2
Pt 3
Pt 4
Pt 5
Pt 6
C
PIM1
PIK3CA
Genetic Alteration
Amplification
Deep Deletion
Mutation
mRNA Upregulation